PHYSICAL REVIEW B VOLUME 36, NUMBER 7 1 SEPTEMBER 1987

## Rapid Communications

*The Rapid Communications section is intended for the accelerated publication of important new results. Since manuscripts submitted to this section are given priority treatment both in the editorial office and in production, authors should explain in their submittal letter why the work justifies this special handling. A Rapid Communication should be no longer than 3½ printed pages and must be accompanied by an abstract. Page proofs are sent to authors, but, because of the accelerated schedule, publication is not delayed for receipt of corrections unless requested by the author or noted by the editor.*

# Valence electronic structure of $Y_1Ba_2Cu_3O_7$

J. A. Yarmoff, D. R. Clarke, W. Drube, U. O. Karlsson, A. Taleb-Ibrahimi, and F. J. Himpsel
*IBM Thomas J. Watson Research Center, Box 218, Yorktown Heights, New York 10598*
(Received 12 May 1987; revised manuscript received 15 July 1987)

The occupied and unoccupied valence-band structure of $Y_1Ba_2Cu_3O_7$ is probed with photoemission, inverse photoemission, and near-edge x-ray absorption. The Cu 3*d* and O 2*p* states nearly coincide, thereby maximizing their interaction. The occupied states are shifted down by 2 eV relative to ground-state band calculations, indicating localization and a Coulomb interaction $U > 2$ eV. The bandwidth is 10 eV with the top of the band at $E_F + 2.5$ eV. Cu is found in the 2+ oxidation state. O has 2*p* holes which are assigned to specific oxygen atoms.

The electronic structure of the copper oxide-based superconductors[1,2] is of considerable interest for understanding the mechanism of superconductivity at high $T_c$. The group of compounds with the highest $T_c$ reported to date is exemplified by $Y_1Ba_2Cu_3O_7$ for which band-structure calculations[3-8] have been reported recently. The calculations indicate a strong electron-phonon interaction but other pairing mechanisms[9] have also been proposed to explain the high $T_c$. Several photoemission studies[10] are in progress. We are using a combination of state-of-the-art techniques such as photoemission, inverse photoemission, and near-edge x-ray-absorption fine structure (NEXAFS) in order to obtain the salient features of the Cu- and O-derived states.

First of all, we note that the Cu 3*d* and O 2*p* states nearly coincide in $Y_1Ba_2Cu_3O_7$, while they are separated by about 3 eV in CuO. This coincidence maximizes the interaction between Cu and O via a resonance effect,[6] leading to strong electron-phonon coupling. The Cu 3*d*, O 2*p* valence band is observed to extend from 7.5 eV below the Fermi level $E_F$ to 2.5 eV above $E_F$. The density of states is distorted relative to ground-state band calculations. All states are shifted away from $E_F$, leaving very low density of states at $E_F$. The center of the occupied states, located at $E_F - 4.5$ eV, has come down by 2 eV. This shift, together with the appearance of satellites below the valence band indicates localization of the Cu-3*d*, O 2*p*-derived states and an on-site Coulomb interaction $U > 2$ eV.

From our NEXAFS results at the Cu and O core edges we obtain the oxidation states of Cu and O, which have been observed to play a critical role for the occurrence of superconductivity. We find that Cu is the 2+ oxidation state and that the 2*p* shell of the oxygen atoms is not filled completely. It is possible to distinguish inequivalent oxygen atoms by their core-level binding energy. The O 2*p* holes are found to be concentrated mainly on the oxygens with low core-level binding energy, which are assigned either to the "one-dimensional" CuO chains or to the BaO planes using different calculations.

The experiments were performed with a photoemission system[11] at the National Synchrotron Light Source and an inverse photoemission system[12] based on a spectrograph. Data were taken at room temperature. The $Y_1Ba_2Cu_3O_7$ was sintered from $Y_2O_3$, BaO, and CuO and

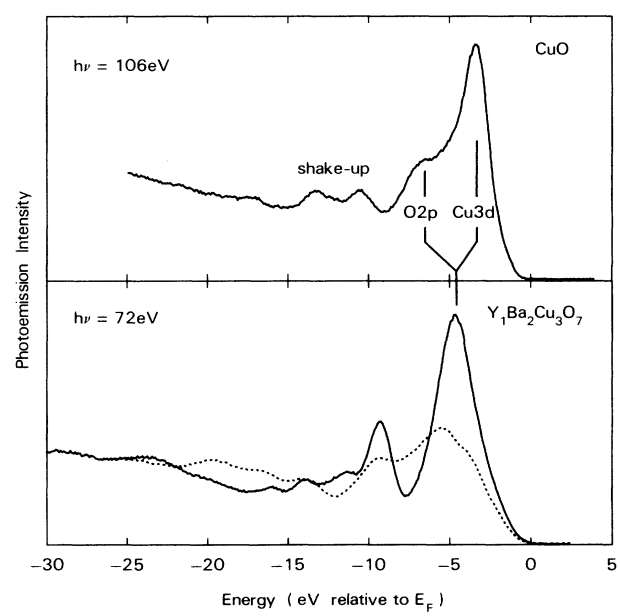


FIG. 1. Comparison of photoemission spectra from $Y_1Ba_2Cu_3O_7$ and CuO. The O 2*p* and Cu 3*d* valence states nearly coincide in the high-$T_c$ material leading to resonantly enhanced Cu-O interaction. The dotted spectrum is from a contaminated sample after oxygen loss caused by irradiation.

 

transferred directly after the last oxygen anneal into a desiccator. From there it was introduced through vacuum interlocks into the spectrometers, avoiding any bakeout in order to prevent loss of oxygen. Clean surfaces were prepared by fracturing in a vacuum of $10^{-10}$ Torr. We find it important to avoid any contact of the samples with water or other solvents since liquids penetrate into these porous materials. Contaminated samples are very sensitive to radiation-induced oxygen loss (see Fig. 1, dotted curve), while samples handled under dry conditions are stable. Even for the dry samples we observe a significant contribution from a thin carbonate overlayer (typically 5 Å) which was identified by its C 1*s* signal. Carbonate gives rise to most of the peak observed at −9.3 eV and contributes to the −4.7-eV peak (see Fig. 1 and compare Ref. 13). It also contributes a large fraction of the O 1*s* core level with higher binding energy (see below). The carbonate ion is mostly associated with Ba since a high binding-energy component of the Ba 4*d* core level increases with higher carbonate concentration. The NEXAFS data are unaffected by the presence of carbonate since secondary electrons with zero kinetic energy (i.e., long mean free path) are detected. We note that carbonate films may cause the weak links that limit the current carrying capacity of high-$T_c$ superconductors. The superconductivity of the samples was characterized by an onset at 97 K and zero resistance at 95 K. X-ray diffraction and optical microscopy showed that the material was single phase.

As a reference, we use spectra from CuO, which is prepared by oxidizing a Cu(100) surface in 10 Torr of $O_2$ at about 400 °C until it turns black.[14-16] In the CuO spectra, one can clearly identify the Cu 3*d* and O 2*p* states at −3.3 and −6.4 eV, respectively (Fig. 1), plus Cu $3d^8$ shake-up satellites[14] at −10.3 and −13.3 eV. In $Y_1Ba_2Cu_3O_7$, by contrast, the Cu 3*d* and O 2*p* states appear to collapse into one peak with a center of gravity at −4.5 eV. A Cu-derived satellite at −13.0 eV is also observed in $Y_1Ba_2Cu_3O_7$ when the photon energy is tuned to the Cu 3*p* resonance ($h\nu \approx 75$ eV).

A summary of the valence-band density of states derived from photoemission and inverse photoemission spectra is given in Fig. 2. The valence band is observed to extend from about 7.5 eV below $E_F$ to 2.5 eV above $E_F$ where a 2-eV band gap (seen as a depression in the inverse photoemission spectrum) separates it from the unoccupied states of the $Y^{3+}$, $Ba^{2+}$, and $Cu^{2+}$ ions. These overall features agree well with first-principles band calculations[3-5] (compare the bandwidth obtained from Ref. 3 indicated by brackets on top of Fig. 2). In order to decompose the valence band into Cu 3*d* and O 2*p* states, we use the photon energy dependence of the photoionization cross section (Fig. 3). Calculated photoemission spectra[3] and our CuO reference spectra show that the O 2*p* states dominate at low photon energies $h\nu$ and, vice versa, the Cu 3*d* states at high $h\nu$. At $h\nu = 41$ eV (full line in Fig. 2) the two cross sections are about equal, and the total density of states is seen. The spectrum at $h\nu = 150$ eV (dotted curve

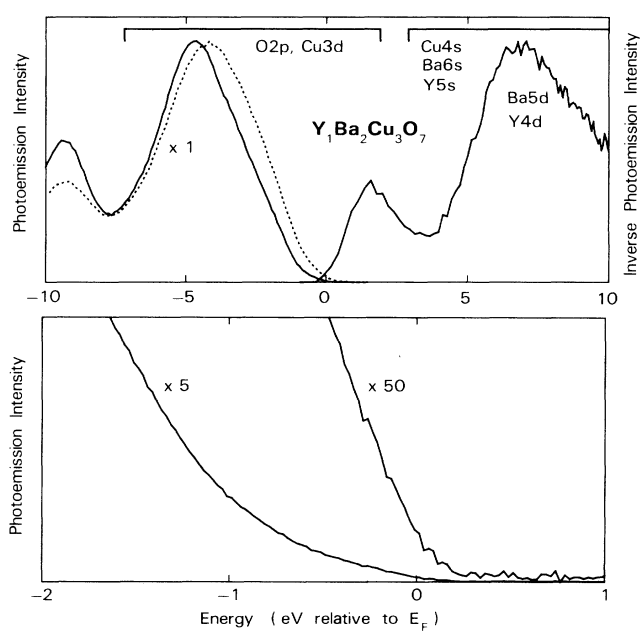


FIG. 2. Density of states for the $Y_1Ba_2Cu_3O_7$ valence band as obtained from photoemission and inverse photoemission. The photoemission spectra at $h\nu = 41$ eV (full lines) represent the total density of states, whereas the spectrum at $h\nu = 150$ eV (dotted line) gives the partial Cu 3*p* density of states. The inverse photoemission spectrum is taken at an initial energy of 18 eV above $E_F$. It emphasizes O 2*p* states. The calculated bandwidth (Ref. 3) is given by brackets. All spectra are normalized to equal maximum height.

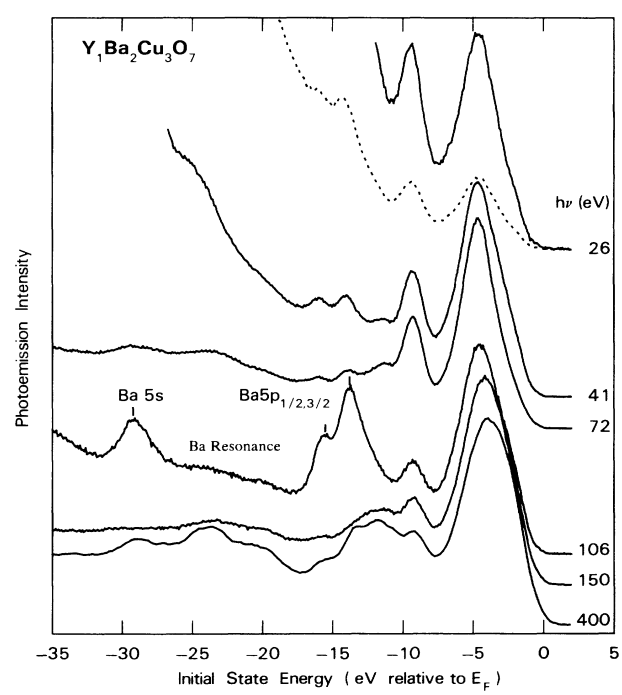


FIG. 3. Photon energy ($h\nu$) dependence of photoemission spectra from $Y_1Ba_2Cu_3O_7$. For $h\nu < 30$ eV, the O 2*p* states dominate; for $h\nu > 100$ eV the Cu 3*d* states dominate. At $h\nu = 106$ eV, the Ba states are enhanced by the Ba $4d \rightarrow$ Ba $4f$ resonance.

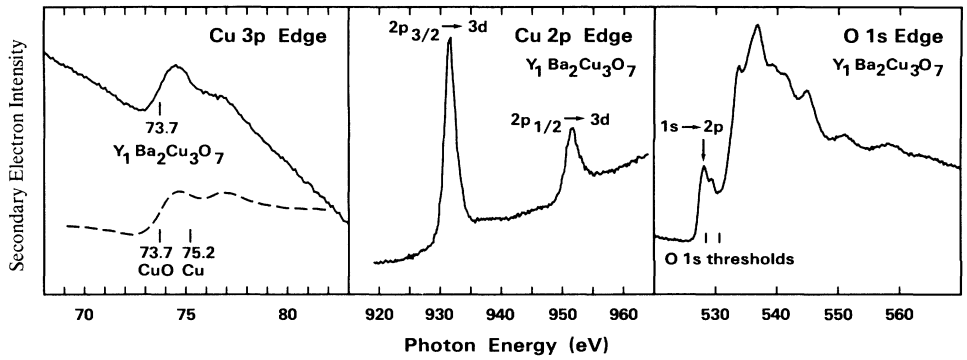


FIG. 4. Near-edge x-ray absorption spectra measured via the yield of secondary electrons. The Cu $3p$ and Cu $2p$ edges are very similar to CuO, indicating $Cu^{2+}$. the O $1s$ edge has a spike at threshold indicating unoccupied O $2p$ states. They are concentrated on the oxygen atoms with lower O $1s$ binding energy.

in Fig. 2) is representative of the high photon energy regime, i.e., it reflects the partial density of Cu $3d$ states. The overall shape of the O $2p$ and Cu $3d$ densities of states is similar except for a small shift of the valence-band peak from $-4.7$ eV at $h\nu=41$ eV to $-4.2$ eV at $h\nu=150$ eV. This near degeneracy of Cu $3d$ and O $2p$ energy levels leads to strong hybridization and large electron-phonon interaction.[6] By utilizing resonance effects we can also project out the Ba-derived states ($h\nu=106$ eV in Fig. 3) which consist of the shallow Ba $5p,5s$ core levels.

The spectral shape of the valence-band photoemission cannot be explained using ground-state band calculations. The center of gravity of the valence states is calculated[3-5] at about 2.5 eV below $E_F$ but observed at 4.5 eV below $E_F$. Furthermore, the photoemission intensity at the Fermi level is very low (about two orders of magnitude smaller than the maximum, see Fig. 2). These discrepancies can be traced to a localization of the Cu $3d$, O $2p$ valence states, which causes incomplete screening. Therefore, a band calculation for the neutral ground state is not appropriate for describing photoemission (and inverse photoemission), which represents a positive (negative) ion state. The incomplete screening of the valence hole in photoemission pulls the states down and causes shake-up satellite emission, as observed. The use of the local density approximation in the calculations may add to this shift. Excited-state effects have been studied for the $3d$ states in Cu by calculating the self-energy. A lowering of the $3d$ bands by a few tenths of an eV is found.[17] By going to Zn, the $3d$ states become more localized than in Cu and the lowering of the $3d$ bands increases[18] to 2 eV. A $3d$ hole was introduced explicitly into excited-state calculations[19] for NiO and a downshift of 2 eV was found due to the Coulomb interaction of the Ni $3d$ states with the hole. The effect of localization and on-site Coulomb interaction $U$ can be described[7-9,20] by model Hamiltonians. In this case the important parameter $U$ can be estimated from our data. The shift of the valence band gives a lower limit of 2 eV for $U$. $U$ could be substantially greater since the large bandwidth of 10 eV quenches the Coulomb shift. Localization could also be responsible for the absence of fine structure in the observed density of states near $E_F$, but strong electron-phonon interaction is another possibility. Already for the "low-$T_c$" $A15$ compounds a phonon broadening in the order of 0.3 eV has been found.[21]

Our NEXAFS results give information about the oxidation states of Cu and O. It is well known that the superconducting properties of $Y_1Ba_2Cu_3O_7$ are sensitive to the oxidation treatment. The valence state of Cu is also important in many models of superconductivity. In a simplified picture, there are two ways to distribute the available electrons among Cu and O, always assuming fully oxidized $1Y^{3+}$ and $2Ba^{2+}$. One needs $2Cu^{2+}+1Cu^{3+}$ per unit cell in order to have $7O^{2-}$. Alternatively, having all Cu atoms in the $2+$ oxidation state would require one oxygen in the $1-$ oxidation state. Our near-edge x-ray absorption data (Fig. 4) favor the second picture, with some spreading of the unfilled O $2p$ states over several oxygen atoms. The Cu $3p$ edge has an energy position identical to that in CuO without additional structures. (The second hump at 77 eV is due to the spin-orbit splitting of the $3p$ core hole; the sloping background in $Y_1Ba_2Cu_3O_7$ comes from valence absorption.) The Cu $2p$ edge behaves likewise (compare Ref. 15 for CuO). The O $1s$ edge is characterized by a spike at threshold (arrow in Fig. 4) which indicates transitions from O $1s$ into unoccupied O $2p$ states. Indeed, the band calculations[3-5] give substantial O $2p$ character for the valence-band states above $E_F$. One may assign the O $2p$ holes to specific oxygen atoms by utilizing O $1s$ core level shifts. We see two O $1s$ levels at binding energies[22] of 530.7 and 528.5 eV below $E_F$ (see O $1s$ threshold bars in Fig. 4). The O $2p$ holes must be concentrated on the oxygen with lower binding energy since more O $1s$ to O $2p$ transitions are observed at the lower threshold than at the higher. An assignment of the two O $1s$ levels to the four crystallographically inequivalent types of oxygen in $Y_1Ba_2Cu_3O_7$ may be made using calculated[3-5] O $1s$ binding energies. One calculation[3] assigns the oxygen atoms with the lowest binding energy to the "one-dimensional" CuO chains, the other[5] to the BaO planes.

Research was carried out in part at the National Synchrotron Light Source, Brookhaven National Laboratory, which is supported by the U.S. Department of Energy, Division of Materials Sciences and Division of Chemical Sciences.

[1]J. G. Bednorz and K. A. Müller, Z. Phys. B **64**, 189 (1986).

[2]M. K. Wu, J. R. Ashburn, C. J. Torng, P. H. Hor, R. L. Meng, L. Gao, Z. J. Huang, Y. Z. Wang and C. W. Chu, Phys. Rev. Lett. **58**, 908 (1987).

[3]S. Massidda, J. Yu, A. J. Freeman, and D. D. Koelling, Phys. Lett. A **122**, 198 (1987); J. Yu, S. Massidda, A. J. Freeman, and D. D. Koelling, *ibid.* **122**, 203 (1987); J. Redinger *et al.* (unpublished); A. R. Freeman (private communication).

[4]L. F. Mattheiss and D. R. Hamann (unpublished).

[5]V. L. Moruzzi (unpublished).

[6]A. R. Williams and J. Kübler (unpublished).

[7]D. M. Newns (unpublished).

[8]P. Lee *et al.* (unpublished).

[9]P. W. Anderson, Science **235**, 1196 (1987); D. Scalapino (unpublished).

[10]M. Onellion *et al.* (unpublished); F. C. Brown *et al.* (unpublished); A. Fujimori *et al.* Phys. Rev. B **35**, 8814 (1987); T. Takahashi *et al.* (unpublished); P. D. Johnson *et al.* Phys. Rev. B **35**, 8811 (1987); R. L. Kurtz *et al.*, *ibid.* **35**, 8818 (1987); Y. Petroff *et al.* (unpublished); S. Hüfner *et al.* (unpublished); A. Schrott *et al.* (unpublished).

[11]D. E. Eastman, J. J. Donelon, N. C. Hien, and F. J. Himpsel, Nucl. Instrum. Methods **172**, 327 (1980); F. J. Himpsel, Y. Jugnet, D. E. Eastman, J. J. Donelon, D. Grimm, G. Landgren, A. Marx, J. F. Morar, C. Oden, R. A. Pollak, and J. Schneir, Nucl. Instrum. Methods Phys. Res. **222**, 107 (1984).

[12]Th. Fauster, D. Straub, J. J. Donelon, D. Grimm, A. Marx, and F. J. Himpsel, Rev. Sci Instrum. **56**, 1212 (1985).

[13]J. A. Connor, M. Considine, and I. H. Hillier, J. Chem. Soc. Faraday Trans. 2, **74**, 1285 (1978); E. Tegeler, N. Kosuch, G. Wiech, and A. Faessler, J. Electron Spectrosc. **18**, 23 (1980).

[14]G. K. Wertheim and S. Hüfner, Phys. Rev. Lett. **28**, 1028 (1972); M. R. Thuler, R. L. Benbow, and Z. Hurych, Phys. Rev. B **26**, 669 (1982); M. Iwan, F. J. Himpsel, and D. E. Eastman, Phys. Rev. Lett. **43**, 1829 (1979).

[15]R. D. Leapman, L. A. Grunes, and P. L. Fejes, Phys. Rev. B **26**, 614 (1982).

[16]T. Robert, M. Bartel, and G. Offergeld, Surf. Sci. **33**, 123 (1972).

[17]F. Sacchetti, J. Phys. F **10**, L231 (1980).

[18]F. J. Himpsel, D. E. Eastman, E. E. Koch, and A. R. Williams, Phys. Rev. B **22**, 4604 (1980).

[19]J. Kübler and A. R. Williams, J. Magn. Magn. Mater. **54–57**, 603 (1986). For another approach, see Ref. 20. It should be noted that NiO is a semiconductor.

[20]J. Zaanen, G. A. Sawatzky, and J. W. Allen, Phys. Rev. Lett. **55**, 418 (1985).

[21]K. M. Ho and M. L. Cohen, Phys. Rev. Lett. **41**, 815 (1978); M. Aono, F. J. Himpsel, and D. E. Eastman, Solid State Commun. **39**, 225 (1981).

[22]The energy calibration of the O 1*s* and Cu 2*p* edges and the O 1*s* binding energies are only accurate to $\pm 1$ eV. The position of the O 1*s* thresholds relative to the absorption edge in Fig. 4 is accurate.